

One-pot synthesis of aromatic nitriles from aldehydes using magnetic material separated from coal fly ash

¹Dhokte AO, ²Sonkamble SG, ¹Lande MK, and ¹Arbad BR*

¹Department of Chemistry, Dr. Babasaheb Ambedkar Marathwada University, Aurangabad, Maharashtra, India.

²Department of Chemistry, Pratishthan Mahavidyalaya Paithan, Dist. Aurangabad, Maharashtra, India.

*Corresponding Author: E-Mail: abr_chem@yahoo.co.in

ABSTRACT

An efficient and simple procedure for the direct synthesis of Aromatic Nitriles from Aldehydes, Hydroxylamine Hydrochloride is described using magnetic material separated from coal fly ash. Coal fly ash is a waste material generated in huge amount by burning of coal for the generation of electricity in thermal power station. It contains SiO₂, Al₂O₃ and magnetic material in significant amounts, from which magnetic material was separated by using magnetic separation method. These separated magnetic material further characterized by XPS, XRD, EDS, FTIR, SEM, TEM and BET techniques. The merits of present method are solvent free reaction conditions, and also excellent yields and short reaction times.

Keywords: Fly ash, Magnetic Material, Aromatic Nitriles.

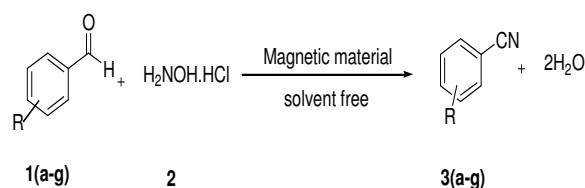
1. INTRODUCTION

Nitriles are key constituents in numerous natural products and a variety of biologically active compounds. [1,2] They are used for preparation of oxazoles [3] tetrazoles [4,5] thiazoles [1] and 2-oxazolines. [6] A number of methods have been reported in the literature for the preparation of nitriles from aldehyde including dehydration of the corresponding aldoximes [7] and using reagents such as oxalyl chloride [8] Burgess reagents [9] [Bis(trifluoroacetoxy)iodo]benzene [10] NH₃/I₂ in tetrahydrofuran (THF)- water [11] NaHSO₄/SiO₂ [12] MeSO₂Cl [13] silica gel [14] and Zeolite [15] and microwave irradiation. [16] Another reported method for nitrile compound synthesis is the one-pot reaction of aldehyde with hydroxylamine using acetyl chloride/charcoal [17] polymer-supported reagent [18] and acetic anhydride. [19] Dewan, *et al.* reported a one-pot conversion of benzaldehyde and hydroxylamine hydrochloride to nitriles using Na₂SO₄ [20] NaHCO₃ [20] Silica gel [21] Montmorillonite K-10 [22] and KSF [22] in dry media under microwave irradiation. Some of these methods suffer from limitations such as corrosive, toxic, expensive or commercially unavailable reagents, excess stoichiometric and no reusability of reagents, vigorous reaction condition, unsatisfactory yields and tedious work up. So, there exists a need for

developing rapid and facile methods for one pot synthesis of nitriles.

Coal fly ash is waste product of coal combustion processes in a coal – fired thermal power stations. Large quantities of coal fly ash are produced in electric power plants throughout the world every year. The amount of coal fly ash formed is approximately 500 million tones per year and likely to increase. The global recycling rate of fly ash is only 15%. [23] It is being consumed in the production of constructions materials, in agriculture, metal recovery, in water and atmospheric pollution control etc. [24] These applications could successful up to some extent to consume part of the huge amount of fly ash. Nevertheless, the search of new applications of the fly ash as either catalyst or as catalyst support material is still ongoing. Literature survey reveals that the fly ash is used as adsorption catalyst for the removal of dyes, [25] heavy metals [26] etc. Major constituents of coal fly ash are SiO₂, Al₂O₃ and Fe₂O₃, Fe₃O₄. After high temperature combustion, these oxides are formed with high thermal stability. Utilization of fly ash for other industrial applications provides a cost effective and environmentally benign way of recycling this solid waste. Currently researchers have focused on how to improve the capability of fly ash through proper beneficiation techniques in order

to increase its catalytic activity. Literature survey reports the catalytic role of activated or modified fly ash for different reactions such as oxidation [27], dechlorination [28], condensation and rearrangement reactions. [29] Fly ash is chemically activated by acid and used for esterification [30] etc. Separation of magnetic material from fly ash is carried out by using magnetic separation method. Magnetic nanoparticles represent a set of unique building blocks whose size and composition are tunable to meet the requirements for a range of applications including magnetic fluids, catalysis, data storage, biomedicine, and toxic waste remediation. [31] The most common methods used to prepare ferrite complex oxides are co-precipitation, sol-gel method, micro-emulsion etc. However, major drawback of these required precursors is the high starting costs of the raw materials that results in high production cost and also traditional process. To overcome these difficulties, the best alternative source is the coal fly ash which is the waste product of coal combustion in thermal power station. In the present work, separated magnetic material is characterized and used as catalyst for a simple, facile synthesis of Aromatic nitriles *via* two component reaction Aromatic aldehydes and Hydroxylamine hydrochloride (Scheme 1).



Scheme - 1: Synthesis of aromatic nitriles using magnetic material as catalyst.

2. EXPERIMENTAL

2.1. Materials

The coal fly ash was obtained from thermal power station, Parli-Vajinath, District-Beed, Maharashtra state, India. Other chemicals used were of synthesis grade reagents (Merck) and used as such, without further purification.

2.2. Isolation of magnetic material from fly ash

The coal fly ash slurry was prepared in clean 500 mL beaker by mixing coal fly ash with deionized water in 1:6 Wt / Vol ratio. The slurry was stirred magnetically using magnetic stir bar for 20-30 minutes, during stirring the magnetic material present in the slurry was attached on the surface of magnetic stir-bar, which was removed and collected several times till the magnetic material was separated completely, which was then dried in an oven at 120 °C for 2h and used as catalytic material.



Figure - 1: photographs of a) coal fly ash b) isolated magnetic material from fly ash

2.3. Catalyst characterization

The X-ray diffraction (XRD) patterns of catalysts were recorded on a Bruker D8 advance X-ray diffractometer using Cu-K α radiation with a wavelength of 1.540 Å. Infrared (FT-IR) spectra were recorded on a FT-IR spectrometer (JASCO, FT-IR, Japan) using dry KBr as a standard reference in the range of 500-4000 cm⁻¹. The scanning electron microscopic (SEM) analyses were carried out with a JEOL JSM-6330 LA operated at 20.0kV and 1.0 nA. The elemental composition of the metal in the fresh fly ash and in magnetic material was estimated using an energy dispersive spectrophotometer (EDS). Brunnauer Emmett- Teller (BET) surface area was carried out on Quanta chrome CHEMBET 3000. X-ray photoelectron spectroscopy (XPS, ESCA-3000-VG, Uckfield, UK) was used to study the chemical composition of the sample. The morphology of material was also characterized with CM-200 PHILIPS transmission electron microscopy (TEM) operated at 200 kV and resolution, 0.23 nm. ¹H NMR spectra of quinoxaline derivatives were recorded on an 200 MHz FT-NMR spectrometer in CDCl₃ as a solvent and chemical shifts values δ (ppm) are recorded relative to tetramethylsilane (Me₄Si) as an internal standard.

2.4. Reaction procedure for synthesis of nitrile

A mixture of an Aromatic aldehydes (2 mmol) and hydroxylamine hydrochloride (2 mmol) and magnetic material (0.1g) were taken in round bottle flask heated at 50-60 °C in oil bath for appropriate time. When reaction was completed, as indicated by TLC, the product was extracted with ethyl acetate and then filtered. The solvent was removed under reduced pressure to afford nitriles.

2.5. Spectroscopic data of compound

4-methoxy benzonitrile (**3b**): IR (KBr) ν_{max} / cm⁻¹ 2937, 2226, 1645, 1606, 1509, 1573, 125; ¹H NMR (CDCl₃, 200 MHz): δ 3.85 (s) 3H, 6.90 (d) J = 6Hz, 2H, 7.60 (d) J = 6Hz, 2H.

3. RESULTS AND DISCUSSION

3.1. EDS analysis

Fresh fly ash and magnetic material was analyzed qualitatively and quantitatively by EDS method are shown in table 1. Magnetically isolated material contains an increased amount of iron (33.86%) as compared to fresh fly ash (4.72%).

Table - 1: Chemical composition of fresh fly ash and magnetic material

Elements	Mass % of Fresh fly ash	Mass % of Magnetic material
O	46.98	34.07
Na	0.25	0.54
Al	15.08	10.92
Si	28.12	20.61
Fe	4.72	33.86
Ca	2.18	-
K	0.94	-
Mg	0.48	-
Ti	1.25	-
Total	100	100

3.2. XRD analysis

X-ray diffraction analysis was performed to understand the morphological nature of the fly ash and magnetic material. Figure 2a shows the XRD pattern for untreated fly ash. It is found that all the reflection peaks at $2\theta = 16^\circ, 20.8^\circ, 23.2^\circ, 26.3^\circ, 30.5^\circ, 33.1^\circ, 36.1^\circ, 39.2^\circ, 40.7^\circ, 42.3^\circ, 45.6^\circ, 50^\circ, 51.9^\circ, 54.5^\circ, 57.4^\circ$ and 59.8° corresponds to the (011), (-111), (-101), (021), (111), (-131), (030), (-230) (-231) (-222), (-240), (-124), (-233) (-250), (015) and (-311) planes and which indicates the crystalline monoclinic nature of fresh fly ash (JCPDS No. 860680) and lattice parameter $a=5.0$ $b=8.6$ $c=8.2$ Å. Whereas (Fig. 2b) shows the XRD pattern for magnetic material and It was found that the sharp reflection peaks at $2\theta = 33.2^\circ, 39.3^\circ, 46.2^\circ, 65.8^\circ, 75.2^\circ, 79.4^\circ, 91.4^\circ, 107.8^\circ, 111.5^\circ$ and 138.4° corresponds to the (104), (006), (007), (118), (217), (1110), (402), (407), (413) and (420) planes which indicates highly crystalline hexagonal structure of ferrite type material (JCPDS No. 860550) and $a=b=5.035$ $c=13.74$ Å.

3.3. Crystallite size determination

The crystalline nature and the crystallite size of the sample was analyzed by X-ray diffraction data. The particle size of the material plays an important role in determining the reactivity of fresh coal fly ash and isolated magnetic material. It was observed that the

particles with smaller size exhibited higher reactivity due to availability of higher specific surface area. [32] Generally, the crystallite size was estimated by Debye-Scherrer equation ($T = 0.94\lambda/\beta\cos\theta$), [33] where T is the particle size, λ is the wavelength, θ is the diffraction angle and β is (FWHM). The mean crystallites size of fresh fly ash is 50 nm and magnetic material is 10 nm.

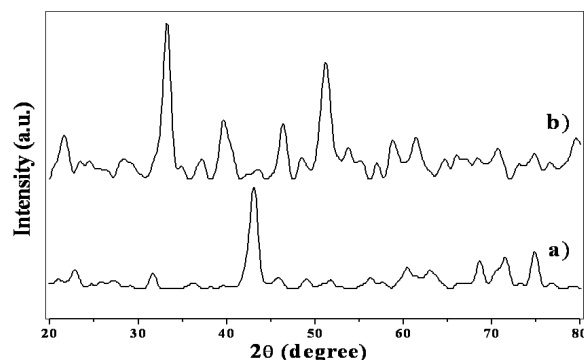
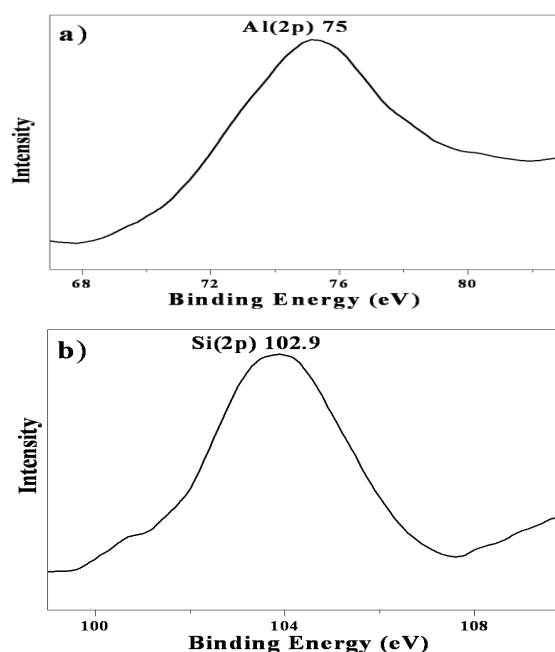


Figure - 2: X-ray diffraction pattern of a) fresh fly ash b) magnetic material.

3.4. XPS analysis

Although the XRD pattern of the samples (Figure 2b) clearly show the hexagonal structure, it is very difficult to exclude the possibility of the γ - Fe_2O_3 phase in the separated magnetic Fe_3O_4 phase similarity. XPS is one of the most effective way to distinguish the two phases because it is very sensitive to Fe^{2+} and Fe^{3+} cations. In (Figure 3c) the levels of $Fe\ 2p_{3/2}$ and $Fe\ 2p_{1/2}$ have binding energies 711 and 720 eV respectively. It conform the presence of Fe_3O_4 phase, [34,35] (Figure 3b) shows binding energy of Si (2p) at 102.9 eV, and (Figure 3a and Fig 3d) shows absorption peaks of Al (2p) and O (1s) are at 74.84 and 531.9 eV respectively.



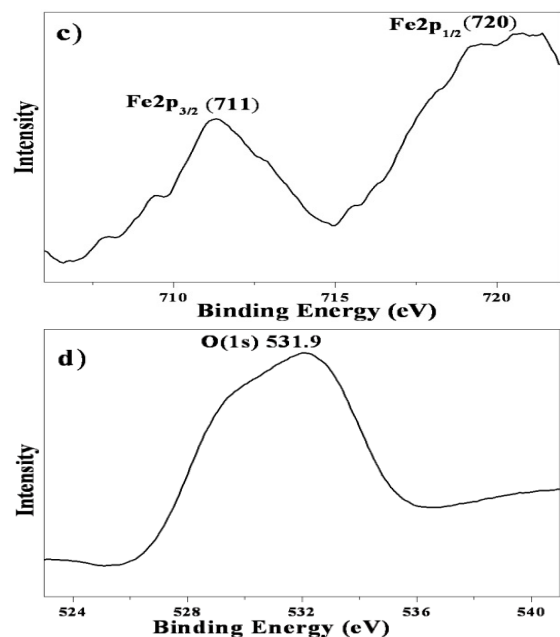


Figure - 3: High-resolution XPS spectra of magnetic material contains a) Al (2p) XPS spectra, (b) Si (2p) XPS spectra, (c) Fe(2p) XPS spectra, and (d) O1s XPS spectra.

3.5. TEM analysis

The TEM images (Figure 4) shows the presence of small spherical particles. From TEM images, measured diameter of particles is ~10 nm, which is consistent with the results of XRD analysis. Electron diffraction pattern of magnetic material (Figure 4d) reveals that the sample is polycrystalline, which can be indexed to the hexagonal structure of magnetic material and accord with the XRD result. TEM image also show that the magnetic material is roughly spherical in shape. Usually, spherical shapes are formed because the nucleation rate, per unit area is isotropic at the interface between the Fe₃O₄ magnetic nanoparticles. [34] Materials are magnetic in nature as well as nano-sized particles are known to have very large surface areas hence, catalytic material will also have high surface energy. Consequently, these fine spherical particles have coated with aluminum silicate network and form aggregated nano-particles. The dark iron center and white aluminum silicate surface of particles are visible.

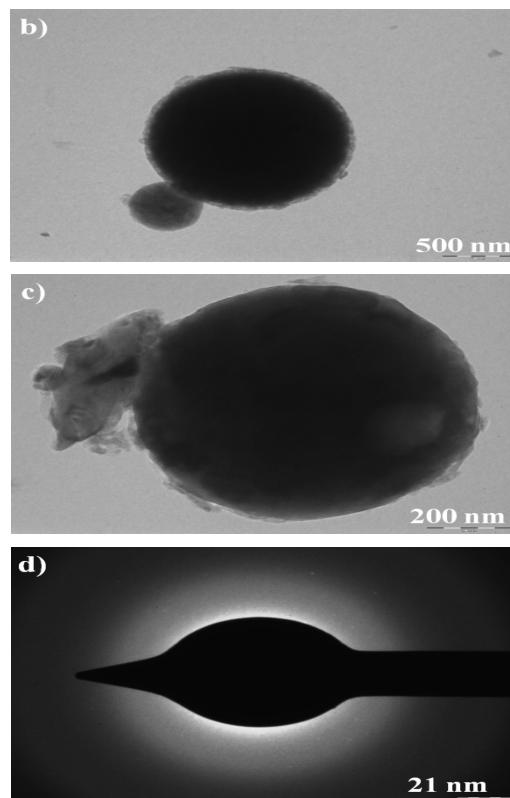
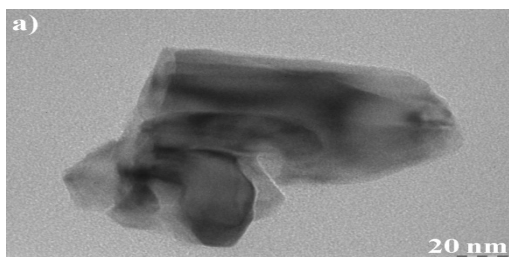


Figure - 4: TEM images (a, b, c) of magnetic material and d) Diffraction pattern of magnetic material.

3.6. SEM analysis

(Figure 5a) SEM image of fresh fly ash shows hollow cenospheres, irregularly shaped, mineral aggregates and agglomerated particles. Similar particles were also observed in other reported micrographs. [31] SEM image of magnetic material (Figure 5b) shows sub-angular and spherical particles, increase in spheroidal nature of the magnetic material due to the magnetic separation method.

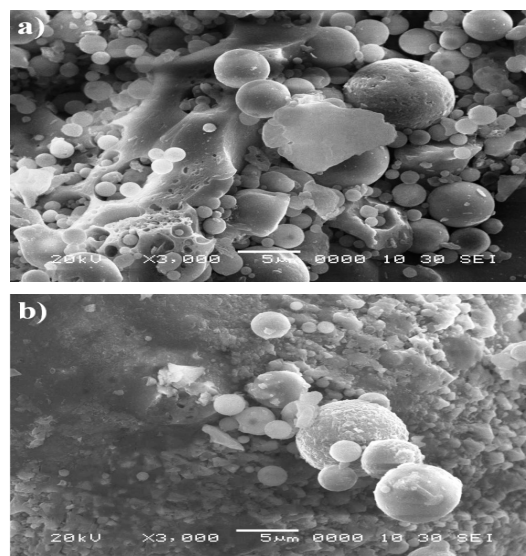


Figure - 5: SEM images of a) fresh fly ash b) magnetic material.

3.7. BET analysis

The specific surface area of fresh fly ash and magnetic material are $1.6233\text{m}^2/\text{g}$ and $105\text{m}^2/\text{g}$ respectively. Thus magnetic material provided surface for reactant to adsorbed and decrease the time to convert reactant to desired product.

3.8. FT-IR analysis

The FT-IR spectrum of fresh fly ash in (Figure 6a) shows a broad band at 1060 cm^{-1} is attributed to Si-O-Si stretching vibrations. (Figure 6b) shows the IR spectrum of magnetic material. The bands absorptions at 1078 , 784 , 560 cm^{-1} , 3437 cm^{-1} and 1634 cm^{-1} . The 1078 cm^{-1} is due to the asymmetric stretching of Si-O-Si bands of the SiO_4 tetrahedron. The 784 cm^{-1} band is composed of the contributions from Si-O-H and Si-O-Fe vibrations, and the band at 560 cm^{-1} is related with the Fe-O stretching. [36,37] The IR spectrum of magnetic material also shows a broad intense band at 3457 cm^{-1} due to hydroxyl groups on the catalyst surface and peak at 1634 cm^{-1} is attributed to bending mode ($\delta_{\text{O-H}}$). [38] It is assumed that during the process of burning of coal at high temperature there is conversion of Fe_2O_3 into Fe_3O_4 which may be coated around aluminosilicate framework. However, these peaks are absent in the FT-IR spectrum of the fresh fly ash (Figure 6a) which do not posses any catalytic activity.

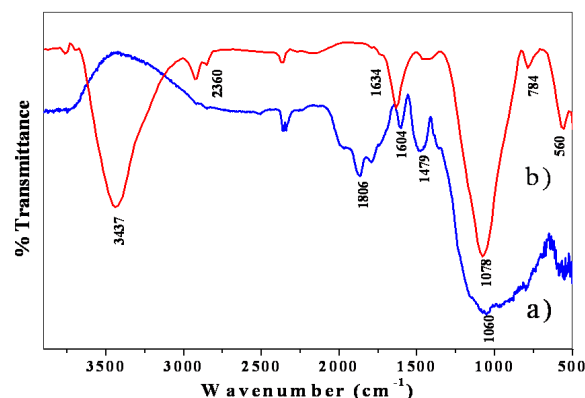


Figure - 6: The FT-IR spectra of a) fresh fly ash b) magnetic material.

3.9. Study of pyridine adsorption:

The probe of our catalyst acidity and basicity was briefly elucidate by pyridine adsorption, which was carried out taking small amount of catalyst and evacuation was done at room temperature for 24 h and second at $150\text{ }^\circ\text{C}$ for 2h. FTIR spectrum of catalyst obtained with evacuation at room temperature (Figure 7a) shows intensive bands at 1536 and 1444 cm^{-1} are

indicating the presence of Bronsted and Lewis acid sites, respectively on catalyst surface, with which pyridine forms coordination bonds. [39,40] However, a third band at 1482 cm^{-1} is widely believed to be the result of a combined contribution of Bronsted and Lewis acid sites. [41] The spectrum also shows bands 3517 , 3610 and 3710 cm^{-1} was due to present of bronsted acidic sites or hydroxyl group on catalyst surface. [42,43] However spectrum (Figure 7 b) obtained after evacuation at $150\text{ }^\circ\text{C}$ for 2h the band 1536 cm^{-1} was disappeared and band 1631 cm^{-1} appear due to the presence of strong proton centers on the catalyst surface, with which pyridine molecules can interact with a creation of Py H^+ . [39-41] The spectrum also shows bands in region $3500\text{-}3700\text{ cm}^{-1}$ was due to present of bronsted acidic sites or hydroxyl group on catalyst surface. Pyridine adsorption study shows that catalyst posses both Lewis acidic sites and Bronsted acidic sites.

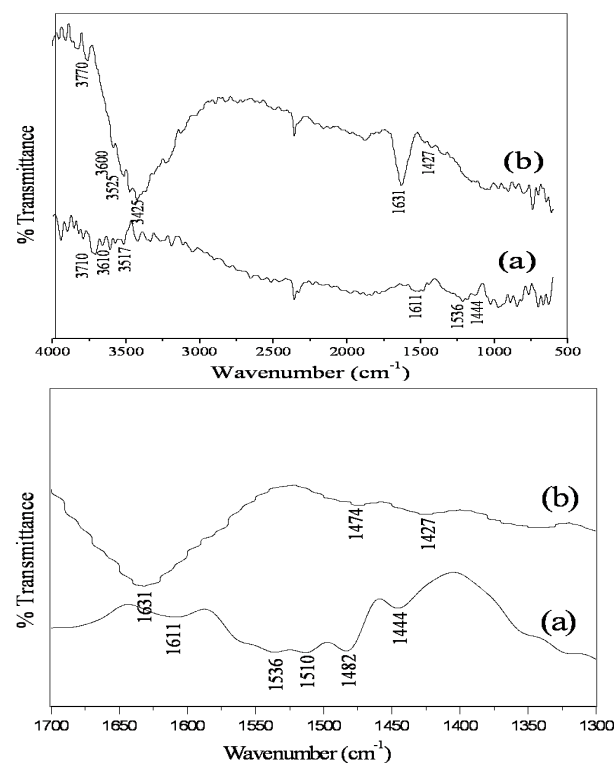


Figure - 7: FT-IR spectrum of pyridine adsorbed on the magnetic material a) at RT and b) at $150\text{ }^\circ\text{C}$.

3.10. Catalytic activity results

Investigations were initiated with 4-methoxy benzaldehyde being chosen as model compound. It was condensed with hydroxylamine hydrochloride in the presence of magnetic material, solvent free condition at $50\text{-}60\text{ }^\circ\text{C}$ in an oil bath using different amounts of catalyst (Table 2). It is observed that 0.1 g catalyst is sufficient for this reaction with 85% yield; increasing amount of catalyst has not shown any enhancement in the

yield. Hence, all the subsequent reactions were carried out under these reaction conditions. A variety of the substituted aromatic aldehydes were converted into nitriles. The reactions were monitored by TLC. The product yield and reaction times are shown in table 3. All the products are known compounds and were identified on the basis of their spectroscopic analyses and by direct comparison of their M.P. with those of the authentic samples. It should be noted that the nitriles were not formed under identical reaction conditions in the absence of the catalysts.

Table - 2: Optimization of the amount of magnetic material for synthesis of nitriles^a

Entry	Amount	Time (min)	Yield (%) ^b
1	Without catalyst	40	No reaction
1	0.05	10	50
2	0.1	3	85
3	1.5	3	85
4	0.2	3	85

^aReaction condition: 4-methoxy benzaldehyde (2 mmol), hydroxylamine hydrochloride (2 mmol), magnetic material 0.1 g, heated at 50-60°C in oil bath; ^bIsolated yield

Table 3 Synthesis of nitriles catalyzed by magnetic material in solvent free condition^a

Entry	R	Time (Min).	Yield (%) ^b	M.P.	
				Observed	Literature
3a	4-Cl	4	90	93-94	95-96 [44]
3b	4-OCH ₃	3	85	57-59	62-63 [44]
3c	4-CH ₃	4	85	215-217	218 [44]
3d	4-OH	4	90	110	110 [22]
3e	2-Cl	5	80	43-46	46-47 [44]
3f	4-NO ₂	4	90	146-149	147 [44]
3g	3-NO ₂	5	75	115-117	115 [44]

^aReaction condition: 1 (2 mmol), 2 (2 mmol), magnetic material 0.1 g, heated at 50-60°C in oil bath; ^bIsolated yield

3.11. Catalyst recovery and reusability

Finally, the recovery and reusability of catalytic material was examined. The catalyst was separated, washed with *n*-hexane, dried at 60°C and activated at 120 °C for 1h before catalytic run. The reusability of the catalyst was examined for the reaction 4-methoxy benzaldehyde and hydroxylamine hydrochloride for three cycles

with almost consistent activity. The results are summarized in table 4.

Table - 4: Reusability of magnetic material in the reaction of 4-methoxy benzaldehyde and hydroxylamine hydrochloride^a

Entry	Cycle	Yield (%) ^b
1	Fresh	85
2	First	85
3	Second	80
4	Third	80

^aReaction condition: 4-methoxy benzaldehyde (2 mmol), hydroxylamine hydrochloride (2 mmol), magnetic material 0.1 g, heated at 50-60°C in oil bath; ^bIsolated yield

4. CONCLUSION

The present procedure using an easily accessible and inexpensive magnetic material as catalyst for the conversion of aromatic aldehydes into nitriles provides a novel protocol. This procedure offers marked improvements with regard to operational simplicity, high yields (75–90%) of products and mild reaction conditions. The catalytic material is easily obtained from the waste of power plants and proved to be efficient catalyst on the basis of conversion of reactants to products, this observation can be used to understand the cost effectiveness of the reaction.

Acknowledgements

The authors are grateful to UGC New Delhi for financial assistances through SAP scheme and the Head, Department of chemistry, Dr. Babasaheb Ambedkar marathwada university, Aurangabad for providing the laboratory facility.

5. REFERENCES

- Chihiro M, Nagamoto H, Takemura I, Kitano K, Komatsu H, Sekiguchi K, Tabusa F, Mori T, Tominaga M and Yabuuchi Y. **J. Med. Chem.** 1995; 38: 353.
- Khanna IK, Weier RM, Yu Y, Xu XD, Koszyk FJ, Collins PW, Koboldt CM, Veenhuizen AW, Perkins WE, Casler JJ, Masferrer JL, Zhung YY, Gregory SA, Seibert K and Isakson PC. **J. Med. Chem.** 1997; 40: 1634.
- Ducept PC and Marsden SP. **Synlett.** 2000: 692.
- Wittenberger SJ and Donner BG. **J. Org. Chem.** 1993; 58: 4139.
- Kadaba PK. **Synthesis**, 1973: 71.
- Jnaneshwara GK, Deshpande VH, Lalithambika M, Ravindranathan T and Bedekar AV. **Tetrahedron Lett.** 1998; 39: 459.

7. Movassagh B and Shokri S. **Synth. Commun.** 2005; 35: 887.
8. Movassagh B and Fazeli A. **Synth Commun.** 2007; 37: 623.
9. Rappai JP, Karthikeyan J, Prathapan S and Unnikrishnan. **Synth. Commun.** 2011; 41: 2601.
10. Telvekar VN, Rane RA and Namjoshi TV. **Synth. Commun.** 2010; 40: 494.
11. Talukdar S, Hsu JL, Chou TC and Fang JM. **Tetrahedron Lett.** 2001; 42: 1103.
12. Das B, Madhusudhan P and Venkataiah B. **Synlett.**, 1999: 1569.
13. Sharghi H and Sarvari MH. **Synthesis**, 2003: 243.
14. Dewan SK and Singh R. **Synth. Commun.** 2003; 33: 385.
15. Hegedus A, Cwik A, Hell Z, Horvath Z, Esek A and Uzsokic M. **Green Chem.** 2002; 4: 618.
16. El-Dusouqui OME, Abdelkhalik MM, Al-Awadi NA, Dib HH, George BJ and Elangdi M.H. **J. Chem.Res.** 2006; 5: 295.
17. Sharghi H and Hosseini Saravi M. **J. Ir. Chem. Soc.** 2004; 1: 28.
18. Baxendale IR, Ley SV and Sneddon HF. **Synlett**, 2002; 775.
19. Lee JC, Yoon JM and Baek JW. **Bull. Korean Chem. Soc.** 2007; 28: 29.
20. Dewan SK, Singh R and Kumar A. **Arkivoc (ii)**, 2006: 41.
21. Dewan SK and Singh R. **Synth. Commun.** 2003; 33: 385.
22. Dewan SK, Singh R and Kumar A. **Synth. Commun.** 2004; 2025.
23. Belardi G, Massimilla S and Massimilla LP. **Resour.Conserv.Cycle.** 1998; 24: 167.
24. Blanco F, Garcia MP and Ayala J. **Fuel**, 2018: 85.
25. Yamada K, Haraguchi K, Gacho CC, Wongsiri BP and Pena ML. Removal of dyes from aqueous solution by sorption with coal fly ash. **In: Proceedings of the international ash utilisation symposium, Lexington, Kentucky, USA.** 2003: 22.
26. Cohen H, Lederman E, Werner M, Pelly I and Polat M. Synergetic effect of coal fly ash as a scrubber to acidic wastes of the phosphate industry. **In: Proceedings of the international ash utilisation symposium, Lexington, Kentucky, USA.** 2003: 20.
27. Zhang AL, Deng FF, Zhou JT, Jin RF, Ling LL and Zhang GL. **Huan Jing Ke Xue.** 2009; 7: 1942.
28. Ghaffar A and Tabata M. **React Kinet Catal Lett.** 2009; 97: 35.
29. Gopalakrishnan M, Sureshkumar P, Kanagarajan V, Thanusu J and Govindaraju RA. **Arkivoc**, 2006; 13: 130.
30. Khatri C and Rani A. **Fuel**, 2008; 87: 2886.
31. Dai Q, Lam M, Swanson S, Rachel Yu R-H, Delia J, Milliron, Topuria T, Jubert PO and Nelson A. **Langmuir**, 2010; 26, 17546.
32. Kimura T. **Micropor. Mesopor. Mater.** 2005; 77: 97.
33. Henry NFM, Lipson J and Wooster WA. The Interpretation of x-ray diffraction photographs, Macmillan, London, 1951.
34. Wensheng Lu, shen Y, xie A and zhang W. **J. magnetism and magnetic mater**, 2010; 322: 1828.
35. Deng X, Lee J and Matranga C. **Surface sci.** 2010; 604: 627.
36. Cristina F, Diniz APP, Viana N and Mohallem DS. **J. of Sol-Gel Sci.and Tech.**, 2005; 35: 115.
37. Zhao L, Yang H, Cui Y, Zhao X and Feng S. **J. Mater Sci.**, 2007; 42: 4110.
38. Mishra BG and Rnga Rao G. **Bull.Mater.Sci.** 2002; 25: 155.
39. Bezrodna T, Puchkovska G, Shimanovska V, Chashechnikova I, Khalyavka T and Baran J. **Applied Surface Sci.**, 2003; 214: 222
40. Akcay M. **J. of Molecular Struc.**, 2004; 694: 21.
41. Seddigi ZS. **React.Kinet.Catal.Lett.**, 2001; 73: 63.
42. Herrero J, Pajares J and Blanco CA. **Clays and Clay Minerals**, 1991; 39: 651.
43. Ravichandran J and Sivasankar B. **Clays and Clay Minerals 1997**; 45: 854. 31.